Journal of Civil Engineering and Urban Planning (2025)
Clausius Scientific Press, Canada

DOI: 10.23977/jceup.2025.070118
ISSN 2616-3969 Vol. 7 Num. 1

Experimental Study on Lateral Impact Resistance of Corrugated Steel Pipe

Li Zhongxiang

Beijing University of Technology, Beijing, 100124, China

Keywords: Corrugated steel pipe; Lateral impact; Impact test; Deformation mode

Abstract: Due to its excellent bending stiffness, lightweight and high strength, and good deformation capability, corrugated steel pipes have been widely used in infrastructure, transportation engineering, and protective structures. With the frequent occurrence of natural disasters and accidents, the impact resistance of corrugated steel pipes under extreme loading has gradually become a research hotspot. To enhance the safety and reliability of corrugated steel pipes under impact loads, this paper systematically conducts experiments on their lateral impact resistance. Through falling hammer impact tests, the effects of different impact energies and hammer head shapes on the deformation patterns and failure mechanisms of corrugated steel pipes are investigated. The time-history curves of impact force and displacement during the impact process are measured experimentally. The mechanical response characteristics of corrugated steel pipes under lateral impact are analyzed. The experimental results show that corrugated steel pipes still possess strong energy absorption capabilities at higher impact energies. Their unique corrugated structure effectively disperses impact loads, reduces local stress concentration, and thereby lowers the risk of structural failure.

1. Introduction

Ripple steel pipes, with their corrugated structure, possess high load-bearing capacity, excellent energy absorption performance, and strong resistance to compression, bending, and impact [1-3]. This makes ripple steel pipes uniquely advantageous in engineering applications that require dynamic loads, impact loads, and extreme conditions. Conducting research on the lateral impact load resistance of ripple steel pipes can not only fill a gap in academic research and promote the development of structural mechanics theory but also effectively address practical engineering issues, enhancing the safety and reliability of infrastructure. It holds significant strategic importance and engineering application value, playing a crucial role in the sustainable development of civil engineering.

In 1896, the United States first initiated research and application of corrugated steel pipe culverts [4]. During World War II, corrugated steel structures were widely used in military fields [5]. It wasn't until the mid-20th century that corrugated steel pipes began to be extensively applied in civil engineering. Due to their axial displacement compensation function and strong lateral stiffness, corrugated steel pipes are primarily used to bear lateral loads, which can be internal or external pressure. Their high external pressure load-bearing capacity makes them particularly suitable for arch structures, such as corrugated steel arch roofs, tunnels, culverts, and integrated utility tunnels.

Currently, developed countries like the United States, Canada, Australia, Japan, and South Korea have established relevant technical standards and production processes for corrugated steel pipes [6,7]. In China, the application of corrugated steel pipes started relatively late [8,9]. Due to limitations in technology and equipment, research and production of corrugated steel pipes once lagged behind. It wasn't until the early 21st century, with the acceleration of urbanization and the proposal of sponge city construction, that corrugated steel pipes gradually gained promotion and application. Especially in areas such as culverts, underground pipelines, and rainwater corridors, the use of corrugated steel pipes has increased significantly. Despite this, due to limited technological accumulation, domestic research and application of corrugated steel pipes are still in the stage of continuous exploration and improvement [10-14].

2. Test plan

2.1 Test piece design and production

This study designed three corrugated steel pipes of the same specifications for impact testing, with specific dimensions shown in Figure 1. The inner diameter of the specimens is 200mm, the nominal diameter is 222mm, the pipe length is 1500mm, the wall thickness is 1.8mm, the wave spacing is 40mm, the wave height is 20mm, and the material used is Q235 steel. The drop hammer impact position is set at the midpoint of the corrugated pipe. Detailed information about the impact test is listed in Table 1, where L represents the clear span of the corrugated steel pipe, H is the impact height, V is the speed of the drop hammer upon impact, M is the mass of the drop hammer, D is the nominal diameter, and t is the thickness.

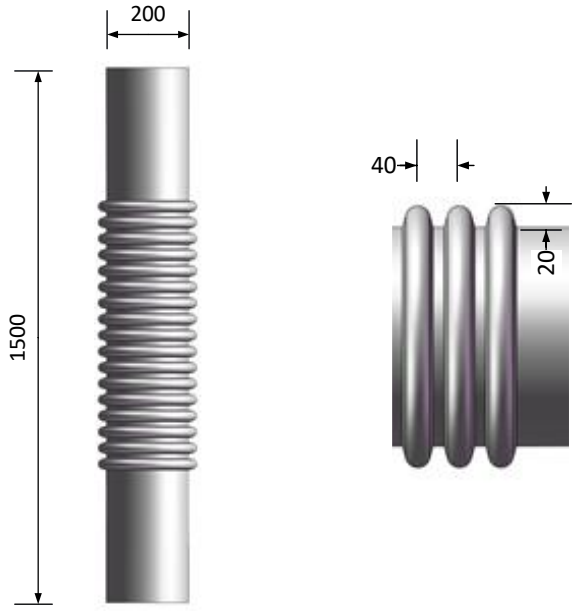

Figure 1 Size of corrugated steel pipe (unit: mm)

Table 1 Impact test information

Test specimen number	L/mm	D/mm	t/mm	M/Kg	H/m	V/m/s	Hammerhead shape
CSP-CM-0.21	720	222	1.8	640	0.21	2.03	cylindrical
CSP-CM-0.40	720	222	1.8	640	0.40	2.80	cylindrical
CSP-SM-0.40	720	222	1.8	640	0.40	2.80	hemisphere

Note: CSP means corrugated steel pipe, C means cylindrical hammer head, S means hemispherical hammer head, M means the impact position is in the middle, 0.21 and 0.40 indicate the impact height.

The manufacturing process of corrugated steel pipes includes key steps such as raw material preparation, forming, welding, corrugation processing, cutting and straightening, and anti-corrosion treatment. First, Q235 steel plates are selected, flattened, and cut, then processed into tubular shapes using a plate rolling machine. High-frequency or submerged arc welding is used to ensure the structural strength and connection stability of the pipe body. Next, a dedicated rolling mill is employed to process the surface of the steel pipe into a corrugated structure, enhancing its stiffness and load-bearing capacity. The forming process is shown in Figure 2. After the corrugation is completed, the steel pipe undergoes cutting and straightening to ensure dimensional accuracy and geometric integrity. Finally, galvanizing, spraying, and other anti-corrosion treatments are applied to improve the corrosion resistance of the steel pipe, meeting the requirements for use in various environments. The final product is shown in Figure 3.

(a) Sample mold (b) roller mill (c) Wave formation process of corrugated steel pipe

Figure 2. Manufacturing process of bellows

Figure 3 Finished corrugated steel pipe

2.2 Loading and measuring device

The impact testing device used in this experiment is the gravity drop hammer impact test system from the School of Civil Engineering, as shown in Figure 4. This system consists of multiple key

components including the drop hammer, crane, slide rail, support frame, enclosure, and control panel, enabling precise impact loading of the test specimen. The drop hammer testing machine releases a pre-set mass of heavy hammer, which falls freely along the slide rail under gravity, impacting the target specimen to simulate the real response behavior of structures or materials under instantaneous impact loads.

The falling hammer impact testing machine is widely used in civil engineering, especially for the study of impact resistance in critical components such as bridges, building structures, pipelines, and offshore platforms. For safety assessments under accidental impacts, explosive loads, or extreme conditions, this equipment can provide genuine experimental data, offering scientific evidence for the design, optimization, and safety evaluation of engineering structures. Additionally, the system can be used to research the performance of high-strength materials, new energy-absorbing structures, and vibration reduction technologies, providing strong support for the development of impact-resistant civil engineering.

To adapt to various testing scenarios and research needs, the equipment is equipped with multiple replaceable hammers to simulate different impact forms and force distributions. For this test, cylindrical and hemispherical hammers with a diameter of 200mm were selected, as shown in Figure 4 (b), for use in different types of impact tests to ensure targeted testing and reliable data. The cylindrical hammer is primarily used to study mechanical responses under concentrated impact, while the hemispherical hammer is better suited for simulating the effects of distributed impact loads, thereby providing a more comprehensive evaluation of the specimen's mechanical properties and failure modes under various impact conditions.

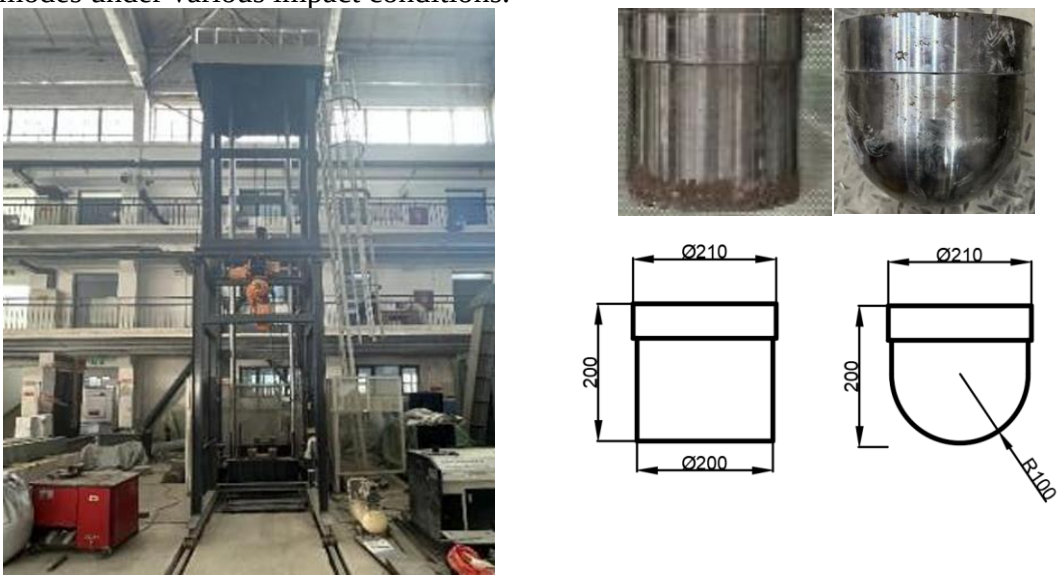

(a) Falling hammer impact tester (b) Two shapes of impact hammer head size

Figure 4 STLH-30000 Falling hammer testing machine

The device is equipped with a data acquisition unit and force sensors (as shown in Figure 5), capable of capturing and recording key physical parameters such as impact force and acceleration during the shock process in real time, providing a solid foundation for precise data acquisition. The data acquisition unit features high-speed sampling and multi-channel measurement capabilities, ensuring accurate recording of mechanical responses at the moment of impact within a short period, and storing experimental data in high-precision digital format for subsequent analysis. The force sensors can monitor and measure the magnitude and trend of impact forces in real time, offering reliable experimental evidence for studying the stress characteristics of materials and structures under instantaneous impact loads.

(A) Collector (b) force sensor

Figure 5 Data acquisition device of hammering system

However, to more comprehensively analyze the response characteristics of specimens under impact loads, it is also necessary to use laser displacement meters and high-speed cameras (as shown in Figure 6). The laser displacement meter can be installed at the bottom of the specimen's mid-span to measure lateral displacement changes under impact. Its high-precision non-contact measurement method can record displacement data in real time, avoiding the potential interference caused by traditional contact sensors on the specimen. Additionally, the high-speed camera captures the entire impact process at ultra-high frame rates during the impact test, providing detailed images of the deformation patterns and local damage under instantaneous impact.

(a) Laser displacement meter (b) High-speed cameras

Figure 6 Data acquisition device

(a) tong hold (b) Steel plugs

Figure 7: Clamping device

To meet the constraint conditions of fixed supports at both ends of the corrugated steel pipe, a rigid chuck and a steel plug were specifically designed and manufactured as shown in Figure 7. The diameter of the chuck is slightly larger than the outer diameter of the corrugated steel pipe to ensure stable clamping during installation, while the diameter of the steel plug is slightly smaller than the inner diameter of the corrugated steel pipe to facilitate smooth insertion into the pipe, thus forming a reliable support structure.

In addition, the support platform of the falling hammer system is made from 80mm thick steel plates, providing extremely high stiffness and load-bearing capacity, which can offer strong support for impact tests. At the same time, the system comes with a platform cover plate, and four bolt holes are set on the front and rear platform plates, which can be fixed with long bolt rods to enhance the restraint effect of the specimen, ensuring the stability of the structure and the reliability of the loading conditions during the test. This design effectively improves the impact resistance of the test platform, making it better suited for high-energy impact tests. The test setup is shown in Figure 8.

(a) Layout diagram of the experimental site

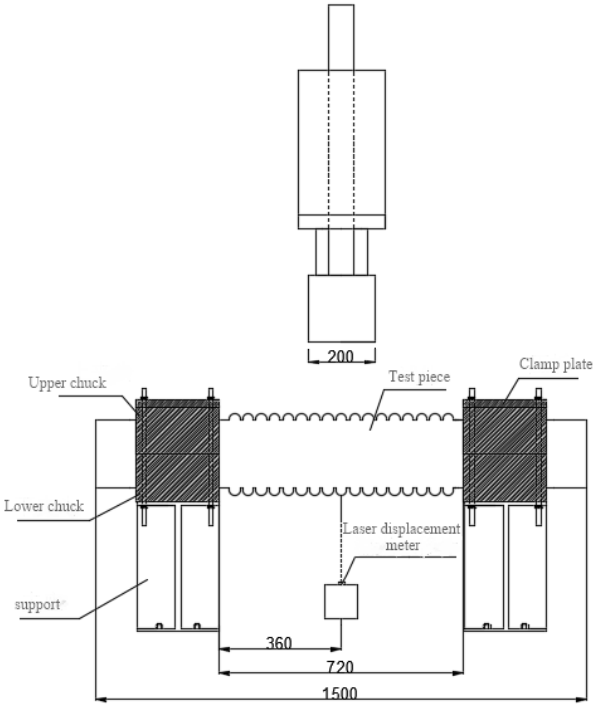

(b) Schematic diagram of the experimental layout

Figure 8: Layout of lateral impact of corrugated steel pipe (mm)

The main data collected in the experiment include the following three categories:

2.2.1 Impact time curve

The impact force is collected in real time by the force sensor of the falling hammer system to record the variation of impact force with time, so as to analyze the stress characteristics of the specimen under the action of impact load.

2.2.2 Transverse displacement time curve

The displacement response at the bottom of the transverse section is measured by a laser displacement meter. It is necessary to ensure that the laser displacement meter is correctly placed at the bottom of the transverse section and that the displacement data during the test does not exceed the measurement range of the equipment to ensure the accuracy and reliability of the measurement.

2.2.3 Impact process video

The whole process of impact test is recorded by high-speed camera, including the fall of the hammer, the impact moment and the deformation evolution of the specimen, which provides intuitive image data support for subsequent test analysis.

2.3 Test operation process

In order to ensure the smooth progress of the impact test and ensure the accuracy and reliability of data acquisition, the test operation process should be carried out in strict accordance with the following steps:

2.3.1 Test piece installation

The operator should position the corrugated steel pipe onto the clamp and carefully adjust its position. This adjustment is crucial to ensure that the hammer head can precisely strike the center of the pipe's span. Subsequently, the operator needs to insert the steel plug into the tube, secure the top plate in place, and tighten the bolt firmly. These steps are taken to guarantee that the specimen is securely fixed and fully meets the test constraint conditions.

2.3.2 Layout of collecting instruments

The operator should install a laser displacement meter at the mid-span of the specimen's underside, ensuring the measurement point aligns precisely with the projected impact area. The technician must properly configure the equipment parameters to prevent the displacement measurements from exceeding the instrument's range. Concurrently, the camera operator should adjust the lens angle to maintain optimal framing of the impact position on the corrugated steel pipe surface. It is crucial to fine-tune both the aperture settings and focal length to ensure the imaging system captures the complete impact event sequence and subsequent specimen deformation with sufficient clarity and detail.

2.3.3 Impact preparation

The impact testing operator should gradually lower the hammer head until it contacts the crown of the corrugated steel pipe to verify impact point alignment. After completing the calibration, the technician must then elevate the hammer assembly to the predetermined drop height and engage the safety retention mechanism in preparation for controlled release.

2.3.4 Data collection

Prior to impact initiation, the testing engineer should sequentially activate the laser displacement meter's measurement module and initialize the high-speed camera's acquisition system, verifying synchronization status through the control interface. The system operator must then actuate the electromagnetic release mechanism on the drop tower, enabling gravitational free-fall of the hammer mass onto the designated specimen area. Upon completion of the impact event, the data monitoring specialist shall immediately execute secure data archiving protocols for both temporal displacement waveforms and visual deformation records.

3. Analysis of test results

This section analyzes the collected test data, including the impact force time curve, displacement time curve, impact process record and deformation mode of the specimen. Through the comprehensive analysis of these data, the dynamic response characteristics of corrugated steel pipe under impact load can be deeply discussed.

3.1 Test piece impact process

The specimen CSP-CM-0.21 was selected for impact process analysis, as shown in Figure 9. The falling hammer dropped freely from a height of 0.21m and generated an impact force upon contact with the corrugated steel pipe, which quickly acted on the specimen. The impact energy was transmitted from the falling hammer to the corrugated pipe, causing localized high stress concentration in the pipe body, but no significant local deformation was observed. Subsequently, the falling hammer moved downward synchronously with the corrugated pipe, and the specimen exhibited overall bending deformation characteristics, with the mid-span displacement continuously increasing and reaching its maximum value at 31ms. During this process, the corrugated pipe effectively absorbed part of the impact energy and stored it in the form of deformation. After the displacement reached its peak, the corrugated pipe and the falling hammer briefly came to a relative standstill for several milliseconds, indicating that the structure has some recovery capability. Following this, under the influence of the material's recovery force and the system's elastic effect [15-17], the corrugated steel pipe began to rebound, gradually lifting the falling hammer. Finally, at 56 ms, the corrugated pipe and the falling hammer completely separated, marking the end of the impact process. This process demonstrates that the corrugated steel pipe not only has strong resistance to local deformation under impact loads but also exhibits certain recovery properties, providing strong support for its application in impact-resistant engineering.

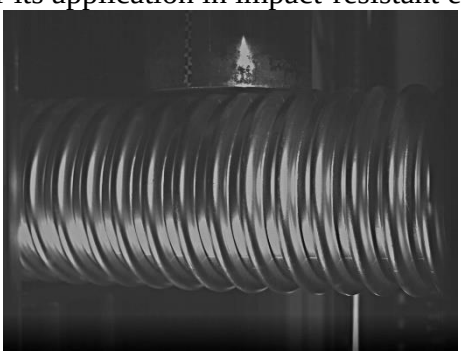

(a) The hammer is about to hit the specimen (0ms)

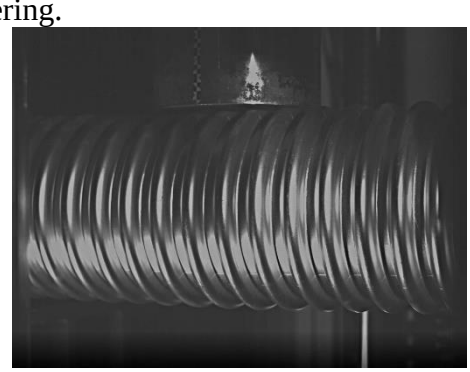

(b) Instantaneous hammer impact on specimen (1ms)

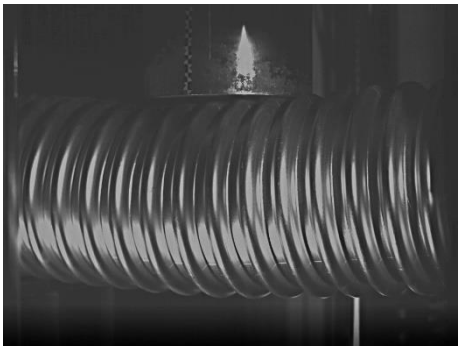

(c) The hammer moves downward with the specimen,
The specimen is bent (7ms)

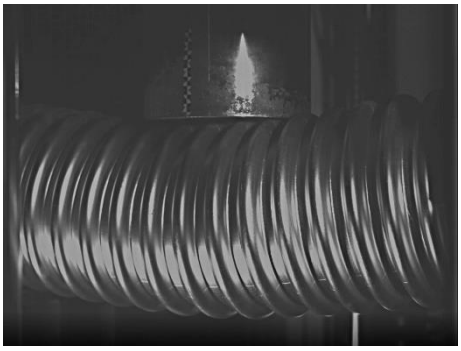

(d) The falling hammer and the specimen span reach their maximum
At the displacement, both are stationary (31ms)

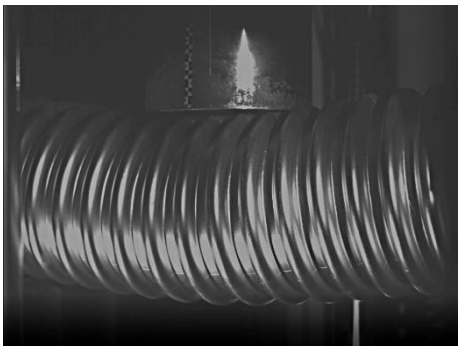

(e) The specimen rebounds upward and both move simultaneously
Upper movement (40 ms)

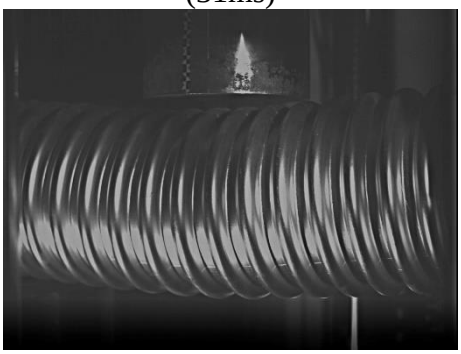

(f) The hammer separates from the specimen and falls
Continue upward motion (56ms)

Figure 9: Process of hammer impact on specimen

3.2 Deformation mode analysis

Figure 10 and Figure 11 show the deformation modes of the corrugated steel pipe components. As can be seen from the figures, under impact loading, the corrugated steel pipe exhibits significant bending deformation, which is consistent with the conclusions of previous studies [18-23]. The dynamic response of the component is significantly influenced by the impact energy; the mid-span displacement increases as the impact height increases. Notably, the local buckling degree of the CSP-CM-0.40 specimen is notably greater than that of the CSP-CM-0.21 specimen. It is worth noting that, from the deformation at the top of the specimens, CSP-CM-0.40 experienced 7 peaks of impact, while CSP-CM-0.21 had only 5 peaks of force. This phenomenon may be due to the higher impact height causing more extensive bending deformation in the corrugated steel pipe, expanding the contact area of the hammer head and thus involving more waves on both sides of the hammer head, thereby increasing the impact affected area.

From the figure, it can be seen that the deformation of the specimen is mainly overall, although there is a certain degree of local deformation as well. However, compared to the whole, its changes are relatively minor. Notably, under the impact of different shaped hammers, the overall deformation of the corrugated steel pipe components is basically consistent, but there are significant differences in local deformation. Specifically, under the impact of a hemispherical hammer, the middle area of the impacted part of the corrugated steel pipe shows more severe indentation, while under the impact of a cylindrical hammer, the indentation is mainly concentrated on the sides of the hammer. This

phenomenon is primarily attributed to the fact that the impact cross-section of the cylindrical hammer is flat. When it acts on the corrugated steel pipe, it causes localized bending deformation, with the central region having the greatest curvature, making the side regions of the corrugated pipe contact the hammer more tightly, thus leading to more pronounced deformation in these areas.

In addition, after the corrugated steel pipe is impacted by a side hammer, its deformation characteristics manifest as follows: the waves at the bottom midsection unfold, while those at both ends fold; conversely, the waves at the top midsection fold, and those at both ends unfold. Moreover, with an increase in impact height, the degree of deformation further intensifies.

a) Overall deformation diagram of CSP-CM-0.21

b) Overall deformation diagram of CSP-CM-0.40

c) Overall deformation diagram of CSP-SM-0.40

Figure 10: Overall deformation of the specimen

① left side ② top ③ offside

a) CSP-CM-0.21 local deformation map

① left side ② top ③ offside

b) CSP-CM-0.40 local deformation diagram

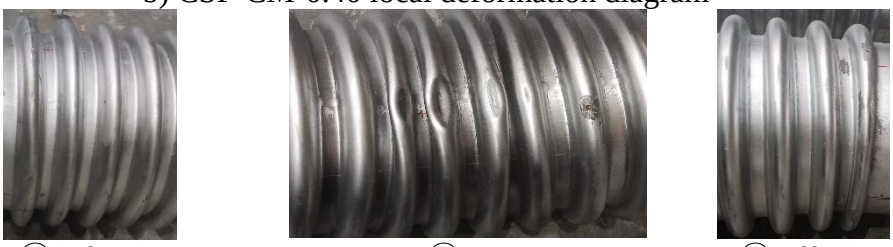

① left side ② top ③ offside

c) CSP-SM-0.40 local deformation diagram

Figure 11: Local deformation of the specimen

3.3 Impact force and displacement time curve

The impact force time curve is measured by the force sensor in the hammering system, as shown in Figure 12. The impact force time curve can be roughly divided into three stages:

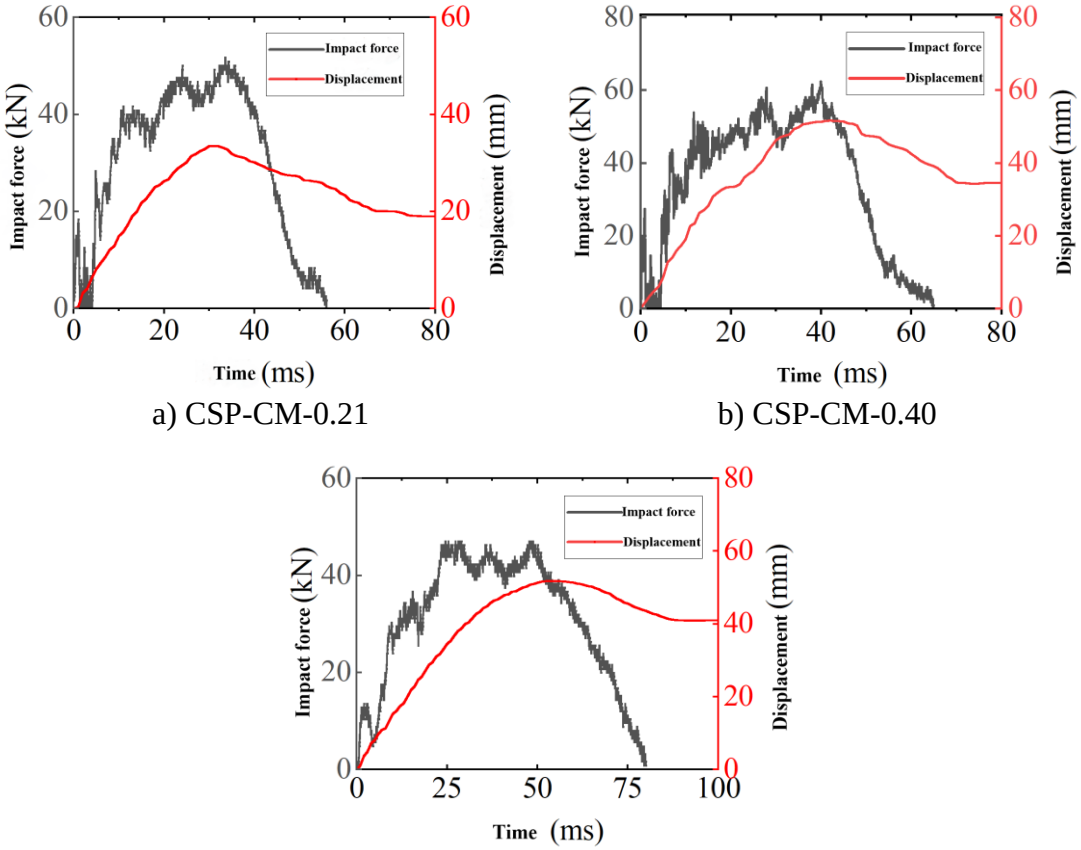

a) CSP-CM-0.21 b) CSP-CM-0.40

c) CSP-SM-0.40

Figure 12: Time history curve of impact force and lateral displacement of the specimen

1) Initial Contact Stage: At the moment of impact between the hammer and the corrugated steel pipe, due to the high instantaneous stiffness of materials and structures, the impact force rises rapidly, forming a brief initial peak. Subsequently, influenced by local buckling effects and constraint conditions, the impact force briefly decreases. During this process, specimens CSP-CM-0.21 and CSP-CM-0.40 experience a brief separation from the hammer head, causing the impact force to

temporarily drop to zero.

2) Impact force growth stage: With the impact deepening, more areas begin to bear the load, and the corrugated steel pipe undergoes overall deformation, and the impact force rises again and finally reaches the maximum value.

3) Energy dissipation stage: When the kinetic energy of the hammer is gradually exhausted, the deformation of the corrugated steel pipe tends to be stable and cannot continue to provide enough reaction force, and the impact force decreases accordingly. Finally, the hammer and the corrugated steel pipe are completely separated, and the impact force drops to 0.

The mid-span displacement curve measured by the laser displacement meter (as shown in Figure 12) indicates that all specimens exhibit similar trends in mid-span displacement, initially increasing to a maximum value, then partially decreasing, and finally stabilizing. This phenomenon is primarily influenced by the combined effects of the falling hammer impact and the specimen's deformation response. In the initial stage, after the falling hammer contacts the corrugated steel pipe, it causes the entire pipe to move downward, leading to a rapid increase in mid-span displacement. As the kinetic energy of the falling hammer gradually dissipates, the bending deformation of the corrugated pipe intensifies until the kinetic energy of the falling hammer reaches zero, at which point the mid-span displacement reaches its maximum value. Subsequently, the corrugated pipe releases some of its elastic potential energy, resulting in a certain degree of rebound in displacement. Ultimately, under the influence of damping effects, the specimen comes to rest, forming residual deformation.

The dynamic responses of corrugated steel pipes under different impact heights are shown in Figure 13. As can be seen from the figure, as the impact height increases, the peak impact force, the peak mid-span displacement, and the duration of the impact all increase. This is because an increase in impact height means more energy is transferred to the corrugated steel pipe when it is struck by the falling hammer, causing the pipe to bear a greater load at the moment of impact, which in turn leads to an increase in the peak impact force. At the same time, higher impact energy requires a longer time to be absorbed, thus increasing the duration of the impact force. Additionally, under higher impact energy, the bending and buckling deformation of the corrugated steel pipe intensifies, further increasing the mid-span deflection and significantly raising the peak mid-span displacement.

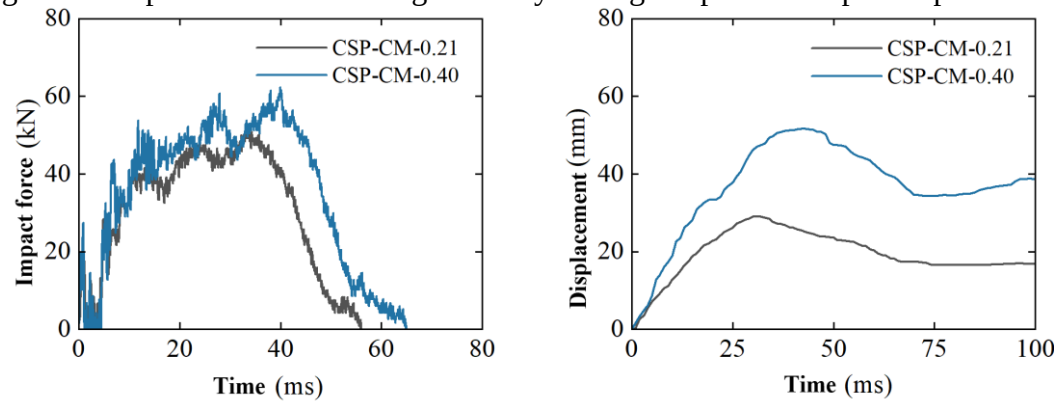

(A) Impulse time history curve

(b) Time history curve of mid-span displacement

Figure 13: Influence of impact height on dynamic response of components

Figure 14 shows the dynamic response of corrugated steel pipes under different hammer head shapes. It can be seen that the peak impact force corresponding to the cylindrical hammer head is significantly higher than that of the spherical hammer head, while the maximum mid-span displacement of the specimens is roughly equivalent. This is mainly because during the impact process, the larger contact area between the cylindrical hammer head and the specimen allows for

greater instantaneous impact force, thus generating a higher peak impact force; whereas the maximum mid-span displacement of the specimen primarily depends on the overall bending stiffness of the corrugated steel pipe, with the hammer head shape having a minor influence. Therefore, the maximum mid-span displacements under the two types of hammer heads are not significantly different.

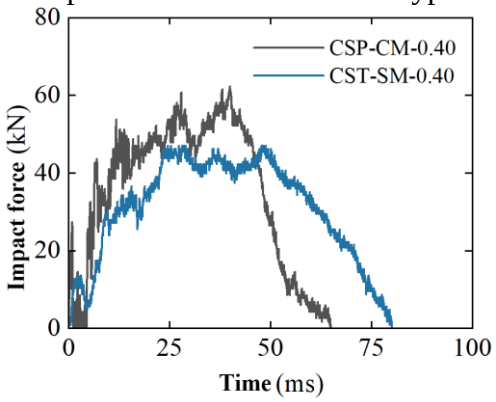

(a) Impulse time history curve

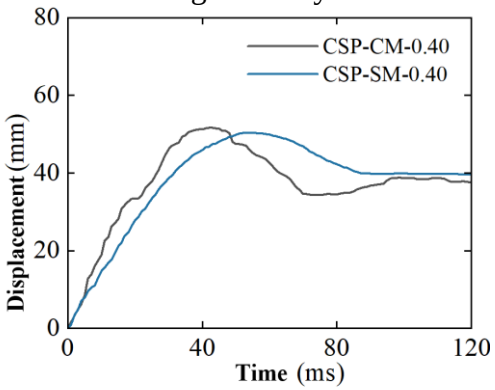

(b) Time history curve of mid-span displacement

Figure 14: Influence of hammer head shape on dynamic response of components

4. Conclusion

(1) Under lateral impact, corrugated steel pipes mainly exhibit overall bending deformation, with local buckling being relatively mild. The greater the impact height, the more wave peaks there are, and the wider the deformation range; the shape of the hammer head affects the characteristics of local deformation, with a cylindrical hammer head causing more pronounced dents on both sides, while a hemispherical hammer head results in more severe denting in the middle.

(2) The impulse time-history curve shows three-stage characteristics of rapid rise, peak, and decline, while the displacement curve exhibits an initial increase followed by partial rebound and eventually stabilizes. The peak impulse force generated by the cylindrical hammer head is higher than that of the hemispherical hammer head, but the displacement responses of both are similar, indicating that the bending resistance of the structure dominates the overall deformation.

(3) With the increase of impact height, the peak impact force, mid-span displacement and impact duration of the specimen all increased significantly, indicating that corrugated steel pipe has a good energy absorption capacity and deformation response with increasing energy. At the same time, the specimen showed a certain rebound after impact, reflecting good recovery ability and toughness.

References

[1] Halmen C, Trejo D, Folliard K. Service life of corroding galvanized culverts embedded in controlled low-strength materials [J]. Journal of Materials in Civil Engineering, 2008, 20 (5):366-374.

[2] Timoshenko S P. Theory of plates and shells [J]. Studies in Mathematics & Its Applications Elsevier Amsterdam, 1959, 6 (3760):606.

[3] ANSI/AISI S100-2007, North American Specification for the Design of Cold Formed Steel Structural Members [S]. Washington, D.C.

[4] Benussi F. and Mauro A. Half-Barrel Shells Composed of Cold-Formed Profiles [P]. Proceeding of IABSE Colloquium, Stockholm, 1986.

[5] EJMA 2015. Standards of the Expansion Joint Manufactures Association [S]. 10th ed., New York: EJMA, INC, 2015.

[6] Meegoda J N, Juliano T M. Corrugated steel culvert pipe deterioration: final report, August 2009 [R]. New Jersey. Dept. of Transportation, 2009.

[7] Corrugated Steel Pipe Institute. Handbook of steel drainage and highway construction products [M]. 2nd ed.

Cambridge: CSPI, 2009.
[8] GB/T34567-2017. Cold bent corrugated steel pipe [S]. Beijing: China Standards Press, 2014.
[9] CECS 167:2004. Technical Specification for Arch Reticulated Steel Roof Structure [S]. Beijing: China Association for Engineering Construction Standardization, 2004.
[10] Zhang Yong. Analysis, design theory and experimental study of metal arched corrugated roof structure [D]. Tianjin: Tianjin University, 2000.
[11] Guo Yanlin and Zheng Haoran. Study on bending and buckling test of color plate corrugated arch roof structure [J]. Industrial Construction, 1997,27 (11): 30-33.
[12] Wang Xiaorong. Theoretical analysis and calculation of three-dimensional corrugated steel plate concrete arch composite structure [D]. Xi 'an: Northwestern Polytechnical University, 2003.
[13] Feng Zhimao. Analysis and design method of soil-structure interaction for earthwork and structure of covered wave corrugated steel plate bridge culvert [D]. Beijing: Beijing Jiaotong University, 2009.
[14] Peng Shuquan. Experimental study and mechanical analysis of corrugated steel plate bridge culvert [D]. Wuhan: Wuhan University of Technology, 2003.
[15] Wu Q, Zhi X, Li Q, Wu Q, Zhi X, Li Q, et al. Experimental and numerical studies of GFRP-reinforced steel tube under low-velocity transverse impact [J]. International Journal of Impact Engineering, 2019, 127: 135-153.
[16] Wang R, Han LH, Hou CC. Behavior of concrete filled steel tubular (CFST) members under lateral impact: Experiment and FEA model [J]. Journal of Constructional Steel Research, 2013, 80: 188-201.
[17] Han LH, Hou CC, Zhao XL, et al. Behavior of high-strength concrete filled steel tubes under transverse impact loading[J]. Journal of Constructional Steel Research, 2014, 92: 25-39.
[18] Zhu A Z, Xu W, Gao K, Zhu A Z, Xu W, Gao K, et al. Lateral impact response of rectangular hollow and partially concrete filled steel tubular columns [J]. Thin-Walled Structures, 2018, 130: 114-131.
[19] Hou CC, Han LH. Life-cycle performance of deteriorated concrete-filled steel tubular (CFST) structures subject to lateral impact [J]. Thin-Walled Structures, 2018, 132: 362-374.
[20] Yousuf M, Uy B, Tao Z, Yousuf M, Uy B, Tao Z, et al. Transverse impact resistance of hollow and concrete filled stainless steel columns [J]. Journal of Constructional Steel Research, 2013, 82: 177-189.
[21] Yousuf M, Uy B, Tao Z, Yousuf M, Uy B, Tao Z, et al. Impact behavior of pre-compressed hollow and concrete filled mild and stainless steel columns [J]. Journal of Constructional Steel Research, 2014, 96: 54-68.
[22] Yang YF, Zhang ZC, Fu F. Experimental and numerical study on square RACFST members under lateral impact loading [J]. Journal of Constructional Steel Research, 2015, 111: 43-56.
[23] Aghdamy S, Thambiratnam DP, Dhanasekar M, Aghdamy S, Thambiratnam DP, Dhanasekar M, et al. Computer analysis of impact behavior of concrete filled steel tube columns [J]. Advances in Engineering Software, 2015, 89:52-63.